Int. J. Electrochem. Sci., 12 **(2017)** 10553 – 10566, doi: 10.20964/2017.11.53

International Journal of
ELECTROCHEMICAL
SCIENCE
www.electrochemsci.org

Simultaneous Sulfide Removal and Hydrogen Production in a Microbial Electrolysis Cell

Zhi-shuai Dong[1], *Yu Zhao*[1*], *Lei Fan*[1], *Yu-xue Wang*[1], *Jun-wen Wang*[1*], *Kan Zhang*[2]

[1] College of Chemistry and Chemical Engineering, Taiyuan University of Technology, Taiyuan, Shanxi, P. R. China, 030024
[2] Institute of Coal Chemistry, Chinese Academy of Sciences, Taiyuan 030001, PR China
[*]E-mail: zhaoyu@tyut.edu.cn, wangjunwen@tyut.edu.cn

Received: 24 July 2017 / *Accepted:* 6 September 2017 / *Published:* 12 October 2017

Sulfide removal and hydrogen production in a microbial electrolysis cell (MEC) were simultaneously accomplished using potassium sulfide as the substrate. Experiments were conducted utilizing a single-chamber MEC under the applied voltage of 0.7 V with different concentrations of potassium sulfide (i.e., 500, 600, 800, and 1000 mg/L). MEC test results indicated that the optimum concentration of potassium sulfide was 600 mg/L with a maximum hydrogen production rate (Q_{H2}) and overall energy recovery (η_{w+s}) of 0.913±0.023 $m^3H_2m^{-3}d^{-1}$ and 261%±6.5%, respectively. The sulfide removal rate was 80.7%. Microbial community analysis of the anode biofilm showed an extensive diversity of bacteria, including *Geobacter*(7.35%), *Desulfurella*(4.31%), *Sulfuricurvum*(3.33%), and *Sulfurospirillum*(2.82%). This study presents a new and effective method for sulfide removal.

Keywords: Sulfide removal; Hydrogen generation; Microbial community diversity; Microbial electrolysis cell

1. INTRODUCTION

Sulfide-rich wastewater is generated by petrochemical processing, as well as paper and digester effluent [1]. Sulfide-containing wastewater should be treated before discharge because it is toxic [2], corrosive [3], and malodorous [4]. Traditional physical chemical methods of sulfide treatment, including precipitation [5-6], absorption [7], and chemical oxidation, are limited by their high costs. Several studies have recently recongnized biological sulfide removal as an alternative method [8]. Microbial full cells (MFCs) are usually used to remove sulfide and generate electricity [9-10]. However, few studies have ever reported on the use of microbial electrolysis cells (MECs) to remove sulfide and generate hydrogen simultaneously.

An MEC contains an anode and a cathode, and the substrate is oxidized in the biofilm on the anode to generate electrons and protons; the electrons pass through the external circuit to the cathode, whereas the protons diffuse to the cathode. Finally, these protons and electrons combine to generate hydrogen at the cathode [11-12]. This feature enables an MEC to generate hydrogen at the cathode, which is accomplished by adding voltage (as low as 0.2 V) over that required for electrolytic hydrogen production (1.23 V in theory). Hydrogen is a promising energy carrier as an alternative fuel because of its high energy density, availability from renewable sources, and zero-emission characteristics [13]. Current hydrogen production methods utilize processes that rely on non-renewable energy sources. Electrohydrogenesis that employs an MEC is a promising approach to produce clean hydrogen fuel from different biodegradable carbon sources, including wastewater and other renewable resources [14]. Lin [15] demonstrated that the sulfide removal rates at 2 and 10 mM Na_2S are 44% and 121% with an applied voltage of 1 V in the MEC.

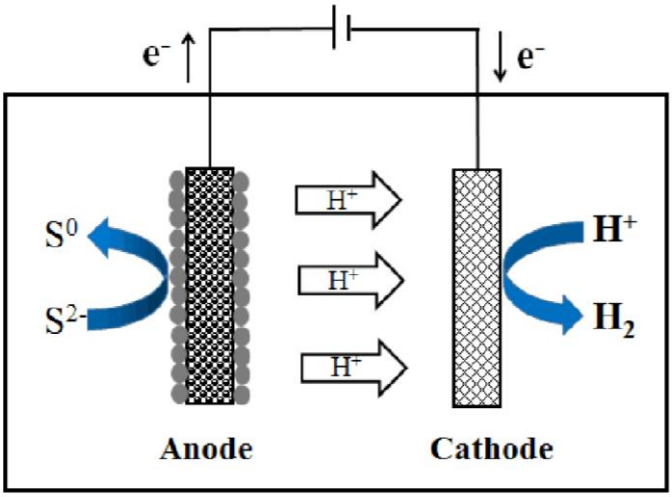

Figure 1. MEC schematic.

Anti-toxicity biofilms were grown in an MFC in this study by increasing the sulfide concentration while lowering the glucose concentration in the same gradient manner until pure sulfide was obtained. The biofilm was adopted as the MEC anode. The sulfide was rapidly oxidized to elemental sulfur (S^0) by sulfide-related bacteria in the biofilm. Potassium sulfide served as the substrate for the MEC with different concentration of potassium sulfide (i.e., 500, 600, 800, and 1000 mg/L) to demonstrate the high sulfide removal and hydrogen production rates.

The sulfide removal in the anode (1) and hydrogen generation in the cathode (2) are expressed in the following equations:

$$S^{2-} \rightarrow S^0 + 2e^- \quad (1)$$

$$2H^+ + 2e^- \rightarrow H_2 \quad (2)$$

2. MATERIALS AND METHODS

2.1. MFC construction and domestication

The two chambers were separated by a proton exchange membrane (Nafion 115, DuPont) with an area of 4 cm^2, and their effective volume was 80 mL. For each MFC, the per-treated carbon felt (2 cm × 5 cm × 1 cm)(Shanghai Lishuo Composite Material Technology Co., Ltd.) was employed as the anode in the anode chamber, whereas the cathode was a platinum network (2 cm × 2 cm) in the cathode chamber. Electrodes were connected with a concealed copper wire. The external circuit was connected to a constant external resistance of 1000 **Ω**. The sludge collected from a local coking wastewater treatment plant in Taiyuan, China served as the inoculated sludge. A 20 mL bacterial solution was injected into the anode chamber of MFC. After each cycle, the anode supernatant was replaced with 60 mL of anode buffer solution and the substrate [16], the cathode buffer solution contained 6.64 $g \cdot L^{-1}$ of $NaH_2PO_4 \cdot 2H_2O$, 20.64 $g \cdot L^{-1}$ of $Na_2HPO_4 \cdot 12H_2O$, 2.634 $g \cdot L^{-1}$ of $K_3[Fe(CN)_6]$. Startup of MFC using 1000 $mg \cdot L^{-1}$ glucose as substrate, domestication of biofilm using glucose and potassium sulfide as substrate, the amount was changed as follows: the sulfide amount increased (100-500 $mg \cdot L^{-1}$), whereas the glucose amount decreased (400-0 $mg \cdot L^{-1}$) in the same gradient manner. The MFCs were operated in batch mode at 25 °C.

2.2. MEC construction

Single-chamber MEC reactors were constructed using a glass cylindrical. For each MEC, the anode was made of carbon felt initially inoculated in the MFCs, whereas the cathode was a platinum network (2 cm × 2 cm). Electrodes were connected with a concealed copper wire, and a power source (HB 17301 SL; Hossoni, Inc., China) was linked to the circuit. The power source provided an external voltage of 0.7 V. After inserting the electrodes, the chamber volume was 100 mL. A 20 mL bacterial solution was injected into the MEC. The gas was collected with a sealed tube glued to the reactor top. The tube top was sealed with a 10 mL gas bag. The nutrient solution contained the following (in 1000 mL distilled water): 5.618 g of $NaH_2PO_4 \cdot 2H_2O$, 6.155 g of $Na_2HPO_4 \cdot 12H_2O$, 0.13 g of KCl, 0.31 g of NH_4Cl, and 12.5 mL of trace metal solution.

The sulfide was added to the nutrient solution of the MFC as an electron donor in the form of K_2S. The MECs were operated in batch mode at 25 °C. The current in the adjacent period reached a stable maximum current under each stable condition, and the MEC was run for at least three cycles. The MEC was operated in the next condition. After each cycle, the supernatant was replaced with 80 mL of nutrient solution, and the cathode was washed to prevent poisoning.

2.3. Analytical methods

The MEC current was recorded every 30 min using a digital multimeter (UNI-T 803; Uni-Trend Electronics Co., Ltd., Shanghai, China). Current density was calculated as $I_m=I/S$, where I is the measured current(A), and S is the anode surface area(m^2). The gas composition and volumetric

fraction of H_2 were determined using a 1000 μL gastight syringe and a gas chromatograph (Thermo Fisher Scientific, Waltham, MA, USA). Micrographs of the biofilm on the anode were investigated under a scanning electron microscope (SEM-7001F, JEOL, Japan).

All electrochemical experiments in this study were performed with a V3 electrochemical workstation (Princeton, USA). A three-electrode system, including a Ag/AgCl reference electrode (MF-2052 Bioanalytical Systems, USA), a Pt net applied as the counter electrode, and a carbon felt biofilm, was employed as the working electrode in an electrolyte of 0.1M phosphate buffer solution (PBS). Linear sweep voltammetry (LSV) measurements were performed at different scan rates in the potential range of -0.6–0V at a scan rate of 10 mV/s. Tafel analysis was conducted to determine the corresponding equilibrium potentials and exchange current density.

Hydrogen recovery, including coulombic efficiency (C_E, %), cathodic hydrogen recovery efficiency (r_{cat}, %), overall hydrogen recovery efficiency (r_{H2}, %), and energy efficiency [i.e., electrical energy input efficiency (η_w, %) and overall energy efficiency (η_{w+s}, %)], were calculated as previously described. Hydrogen production rates (Q_{H2}, $m^3H_2m^{-3}d^{-1}$) were also described. This formula showed in Supporting Information.

Sulfide concentration was determined by an ion-selective glass electrode (Cole Parmer, Chicago, IL) in accordance with the Standard Methods for the Examination of Water and Wastewater [17].

2.4. 16S rRNA

After running in the MEC for 6 months, the carbon felt was cut and crushed using a sterile spatula. Microbial samples were obtained from the surface of the carbon felt and sludge. Total community genomic DNA extraction was performed with an E.Z.N.A.Soil DNA Kit D5625-01 (Omega, USA) in accordance with the manufacturer's instructions. We measured the DNA concentration with a Qubit 2.0 (life, USA) to ensure that adequate amounts of high-quality genomic DNA have been extracted.

Polymerase chain reaction (PCR) was started immediately after the DNA was extracted. The 16S rRNA V3–V4 amplicon was amplified utilizing a KAPA HiFi Hot Start Ready Mix (2×) (TaKaRa Bio Inc., Japan). Two universal bacterial 16S rRNA gene amplicon PCR primers were applied: the amplicon PCR forward primer (CCTACGGGNGGCWGCAG) and amplicon PCR reverse primer (GACTACHVGGGTATCTAATCC).

After amplification, the PCR products were purified with AMPure XP beads. The samples were delivered to Sangon BioTech (Shanghai) for library construction using a universal Illumina adaptor and index. Before sequencing, the DNA concentration of each PCR product was determined with a Qubit® 2.0 Green double-stranded DNA assay and it was quality controlled with a bioanalyzer (Agilent 2100, USA). Depending on the coverage requirments, all libraries can be pooled for one run.The amplicons from each reaction mixture were pooled in equimolar ratios based on their concentration. Sequencing was performed with the Illumina MiSeq system (Illumina MiSeq, USA) in accordance with the manufacturer's instructions.

3. RESULTS AND DISCUSSION

3.1. Anti-toxicity biofilm domestication

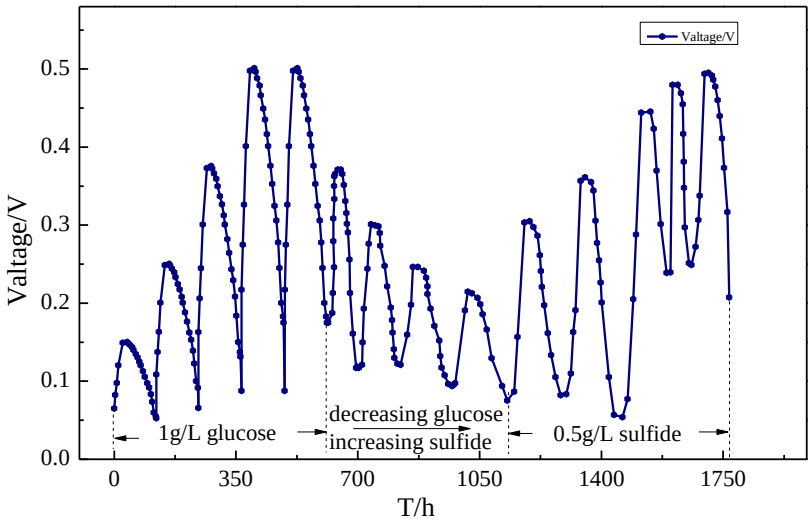

Figure 2. Startup of MFC using 1000 mg·L^{-1} glucose as the substrate and voltage generation of anti-toxicity biofilm domestication in the MFC.

The voltage profiles of MFC with different substrates are illustrated in Fig.2. The output voltage increased rapidly until it reached a stable voltage when the medium was refreshed after approximately 20–30h and then decreased. The voltage output reached 149 mV at 24 h, 250 mV at 158 h, 376 mV at 279 h, 510 mV at 390 h, and 510 mV at 514 h. Thus, the start-up time of 1000 Ω external resistors was 390 h. The substrate amount was changed as follows: the sulfide amount increased, whereas the glucose amount decreased in the same gradient manner. When the substrate concentrations of sulfide and glucose were 100 and 400 mg·L^{-1}, respectively, a stable voltage generation of 371 mV was attained. When the substrate concentrations of sulfide and glucose were 200 and 300 mg·L^{-1}, respectively, a stable voltage generation of 300 mV was attained. When the substrate concentrations of sulfide were 300, 400, and 500 mg·L^{-1}, a stable voltage generation of 246, 215, and 305 mV was attained, respectively. The experiments were repeated twice, and the output voltage reached the maximum value of 495 mV.

3.2. Effects of current density in the proposed MECs

After running in MEC, the sulfide performance as a substrate (the concentration was 500 mg·L^{-1}) became stable at the current density. In Fig.3, when the sulfide substrate concentration was 500 mg·L^{-1}, the current density reached its maximum value of 5.42 A·m^{-2} within the first 0.5 h of operation and then decreased gradually until the cycle end (24.5 h). The experiments were performed twice after a cycle. The peak current density at the third cycle was 5.44 A·m^{-2} when the medium replacement was only 0.02 A·m^{-2} higher than that of the first cycle, which indicates the excellent stability of the

performance. Under the sulfide substrate concentration of 600 mg·L^{-1}, the current density curve was similar to that the sulfide substrate concentration of 500 mg·L^{-1}.

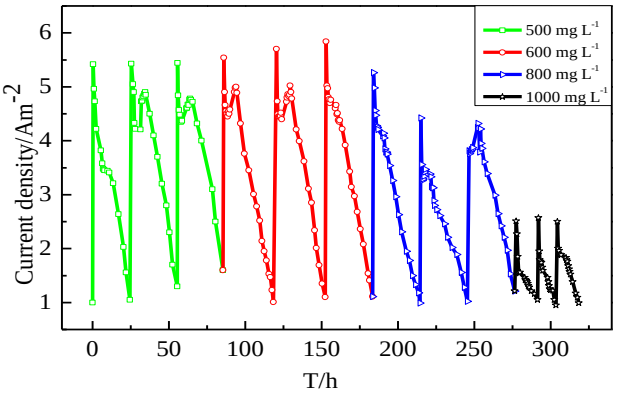

Figure 3. Current density variation with time in a cycle of the MEC at different concentrations of sulfide with an applied voltage of 0.7V.

The current density reached its maximum value of 5.7±0.16 A·m^{-2} after the medium was replaced and then rapidly decreased because of the medium consumption (approximately 33 h). The peak current density and cycle time of the sulfide substrate concentration was 600 mg·L^{-1}, which was slightly higher than 500 mg·L^{-1}, which may be attributed to the 600 mg·L^{-1} of the sulfide being the most beneficial to the bacterial activity. When the sulfide substrate concentration was 800 mg·L^{-1}, the current density became stable and reached its maximum value of 4.42 A·m^{-2} simultaneously. The time required to reach this value increased to approximately 6 h, and the running time was 30.5 h. When the medium was 1000 mg·L^{-1} of sulfide, the current density significantly decreased. The stable and maximum value reached 2.53±0.4 A·m^{-2} after the medium was replaced at approximately 1 h, but the time cycle was only 14 h. This result may be due to the sulfur ion concentration being excessively high that inhibits bacterial activity or Pt poisoning [18].

3.3. Sulphide removal

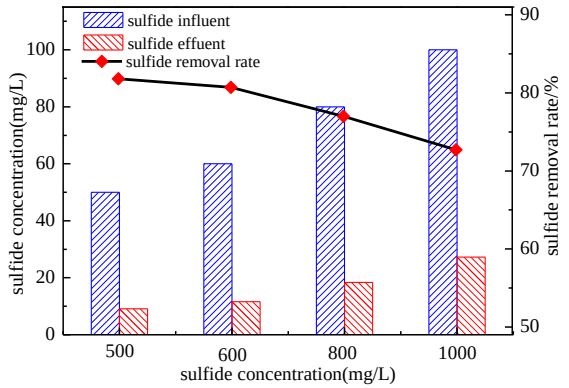

Figure 4. Variations in the sulfide concentration in the influent and effluent, as well as the sulfide removal rate with different sulfide substrate concentrations.

Table 1. Comparison of the sulfide removal rate for the different sulfide substrate concentrations and other initial sulfide concentrations under different power supply levels.

Initial concentration ($mg \cdot L^{-1}$)	Voltage (V)	Time (h)	Sulfide removal rate (%)	Reference
156	1.0	48	44	[15]
780	1.0	48	121	[15]
60	–	–	58.3	[19]
100	–	72	84.7	[20]
546	–	120	47.1	[21]
500	0.7	24.5	81.8	Current study
600	0.7	33	80.7	Current study
800	0.7	30.5	77	Current study
1000	0.7	14	72.7	Current study

Changes in the removal rate of sulfide in the catholyte are shown in Fig.4. The effects of the initial sulfide concentration (i.e., 500, 600, 800, and 1000 $mg \cdot L^{-1}$) with different cycle times (i.e., 24.5, 33, 30.5, and 14 h) on the MEC performance were investigated. When the sulfide substrate concentration was 600 $mg \cdot L^{-1}$, the sulfide concentration decreased with time, whereas the sulfide concentrations decreased from 500 $mg \cdot L^{-1}$ to 91 $mg \cdot L^{-1}$ until the cycle end at approximately 24.5 h. Correspondingly, the sulfide removal rates with 600, 800, and 1000 $mg \cdot L^{-1}$ reached 80.7%, 77%, and 72.7%, respectively, which demonstrate that MEC was promising for sulfide wastewater treatment. Sulfide can be rapidly oxidized to other sulfur compounds through electrochemical and biological actions in the anode compartment [20]. In contrast to previous studies, we used MEC to handle ultra-high concentrations of sulfide and obtained hydrogen.

3.4. Hydrogen production and energy recovery

The gas produced in the experiments was collected, and its composition was analyzed (Fig.5A). The gas produced at the sulfide substrate concentration of 600 $mg \cdot L^{-1}$ for the MEC in one cycle was 20.1±0.5 mL, which was 39.3% higher than that at 800 $mg \cdot L^{-1}$ for the MEC (12.2±0.3 mL) at the cycle end and 65.7% higher than that at 500 $mg \cdot L^{-1}$ (6.9±0.2 mL) at the cycle end. The sulfide substrate concentration of 1000 $mg \cdot L^{-1}$ could only collect 4±0.1 mL in one cycle. The gas composition produced at the sulfide substrate concentration of 500 $mg \cdot L^{-1}$ for the MEC included H_2 (98.17%±3.1%), CH_4 (0.25%±0.1%), and CO_2 (1.57%±0.4%).

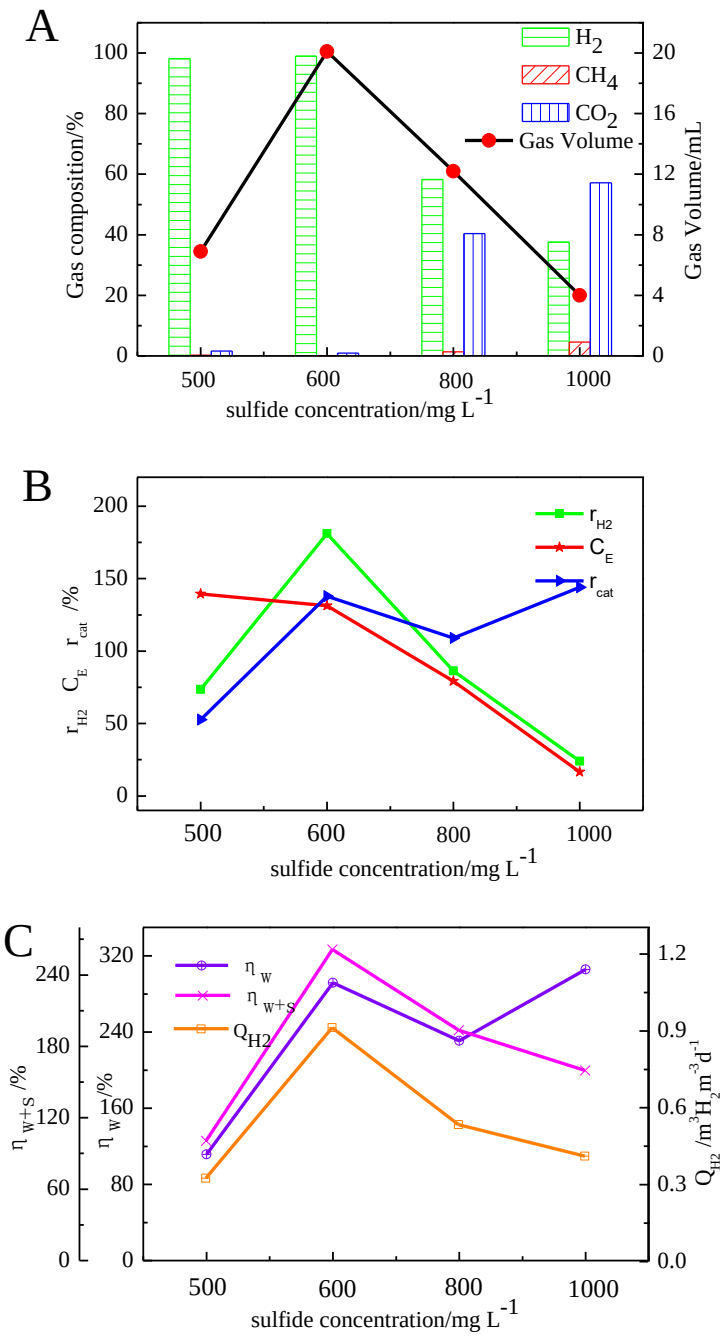

Figure 5. Gas composition and volume (A), hydrogen recovery efficiencies (B), and hydrogen production rates and energy recovery efficiencies (C) with different sulfide substrate concentrtions.

The H_2 and CH_4 gas compositions produced at the sulfide substrate concentration of 600 mg·L^{-1} totaled 99.02%±2.8% and 0.07%±0.01%, respectively, which were higher than those of the 500 mg·L^{-1} sulfide substrate. The gas composition produced at the sulfide substrate concentration of 800 mg·L^{-1} included H_2 (58.23%±1.5%), CH_4 (1.33%±0.2%), and CO_2 (40.38%±0.5%). The H_2 proportion significantly decreased, whereas the CH_4 and CO_2 proportions significantly improved.

Fig.5B shows that the coulombic efficiencies (C_E) at sulfide substrate concentrations of 600 and 800 mg·L^{-1} reached 131% and 79.2%, respectively, which were higher than that at 500 mg·L^{-1}

(139%) and 1000 mg·L^{-1} of sulfide substrate (16.6%). The C_E values exceeded 100%, which indicate that electron recycling occurred by the bioanode using hydrogen as an electron donor [22-23]. The cathodic hydrogen recoveries (r_{cat}) at sulfide substrate concentrations of 600, 800, and 1000 mg·L^{-1} were above 100%, which suggest that more hydrogen was recovered than expected based on the current.

The nature of the hydrogen production rates and energy efficiencies are described in Fig.5C. The maximum hydrogen production rate (Q_{H2}) at a sulfide substrate concentration of 600 mg·L^{-1} (0.913±0.023 $m^3H_2m^{-3}d^{-1}$) was comparable with those at 800 mg·L^{-1} (0.534±0.013 $m^3H_2m^{-3}d^{-1}$) and 1000 mg·L^{-1} (0.411±0.010 $m^3H_2m^{-3}d^{-1}$), whereas it was superior to that at 500 mg·L^{-1} (0.325±0.009 $m^3H_2m^{-3}d^{-1}$). The electrical energy input efficiencies (η_w) were 112%±3.2% (500 mg·L^{-1} of sulfide as substrate), 292%±7.3% (600 mg·L^{-1} of sulfide as substrate), 231%±5.7% (800 mg·L^{-1} of sulfide as substrate), and 306%±7.6% (1000 mg·L^{-1} of sulfide as substrate), which indicates that sufficient hydrogen was produced to power the MEC. The relatively high values of η_w are due to the low current densities output [24]. These results can be translated into higher energy recovery from wastewater [25].

3.5. Electrochemical properties

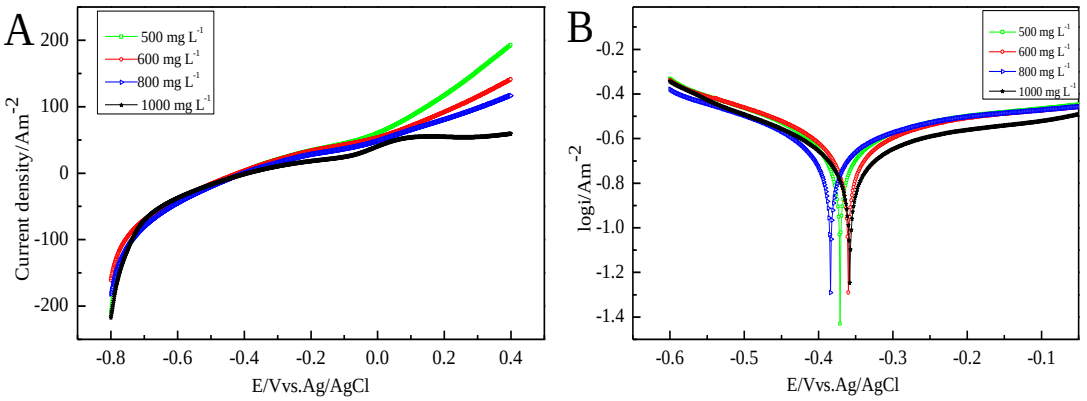

Figure 6. LSV curves (A) and Tafel plots(B) for the different sulfide substrate concentrations with the presence of an anode at a scan rate of 10 mV/s in neutral phosphate buffer. The inset figure shows the LSV and Tafel at the end of the three-cycle MEC work.

The use of different sulfide substrate concentrations of the anode biofilm generated different electrochemical properties. The LSV curves of the anode biofilm domesticated by the different sulfide substrate concentrations are shown in Fig.6A. Increasing the sulfide substrate from 500 mg·L^{-1} to 1000 mg·L^{-1} decreased the current density from 34.2 A m^{-2} to 18.13 A m^{-2} at -0.2 V. However, the acclimated biofilm produced a current density of 33.4 A m^{-2} when the sulfide substrate concentration was 600 mg·L^{-1}, which was lower than the 34.2 A m^{-2} at 500 mg·L^{-1}. When the sulfide concentration were 500, 600, 800, and 1000 mg·L^{-1}, the acclimated biofilm produced current densities of 193, 141, 117, and 59.33 A m^{-2}, respectively. The corrosion behavior investigated by the Tafel plots is shown in Fig.6B. The exchange current density at the sulfide substrate concentration of 600 mg·L^{-1} (3.279 mA) exceeded those at the three other concentration (i.e., 3.105 mA for 500 mg·L^{-1}, 3.101 mA for 800

mg·L^{-1}, and 2.186 mA for 1000 mg·L^{-1} of sulfide substrate). The higher corrosion rate promoted more cells on the surface, which may promote electron transfer from the bacteria to the electrode [26].

3.6. Scanning micrographs

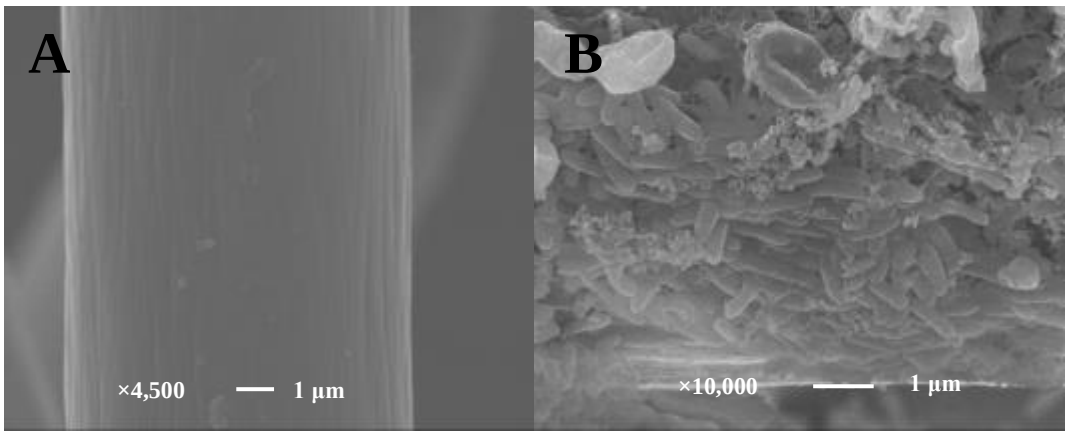

Figure 7. SEM images of the bare carbon felt (A) and microbes on the anode surface at the sulfide concentration of 1000 mg·L^{-1} at the end of the three-cycle MEC work (B).

Fig.7 reveals the microbial images of the growth on the bare carbon felt. The structure of the carbon felt without cells was initially bare (Fig.7A). After the four sulfide substrate concentrations for the biofilm domestication were introduced, the biofilm formed on the carbon felt surface was no longer uniformly distributed (Fig.7B). Under the sulfide substrate concentration of 1000 mg·L^{-1}, some chain-like and ring-like bacteria were attached to the surface. The increasing sulfide concentrations resulted in more microbes on the carbon felts because the microbes adapted to the sulfide-containing environments. More sulfide-related and producing-electricity bacteria that adhere on the carbon felt may be introduced, which increases the biodiversity. This scenario is a further reminder of the 16S rRNA complicon sequencing results. Differences in the sulfide substrate concentrations may present selectivity toward different types of bacteria, which could lead to anodes with markedly different electrical properties.

3.7. Microbial community analysis

Table 2. Number of sequence reads after quality filtering, operational taxonomic units (OTUs) at 95% sequence identity, and diversity indices of the bacterial community in two samples collected from the inoculum and the MEC.

Sample	Total # of quality filtered sequence reads	OTUs	Coverage	Shannon diversity index	Simpson index	Chao1 index	ACE index
Inoculum	11488	977	0.95	4.46	0.07	2249	3293
MEC	81814	5269	0.95	5.27	0.02	41123	87394

In this study, the number of sequence reads after quality filtering, OTUs at 95% sequence identity, and diversity indices of the bacterial community in two samples collected from the inoculum and MEC were compared (Table 2). The microbial community distributions in the inoculum and MEC were investigated with 16S rRNA complicon sequencing (Fig.8). A total of 84,564 raw sequence reads were produced in this study through the high-throughput amplicon sequencing of the 16S rRNA gene (V3–V5 region) in the biomass sample of the anolyte in the MEC, which contains 100 mg of sulfide in a 100 mL buffer solution. By contrast, 15,389 raw sequence reads were generated in the biomass sample of the inoculum. After quality filtering, 11,488 sequence reads were continued for further analysis of the inoculum sample, whereas 81,814 sequence reads were continued for further analysis of the MEC sample. These results suggest that the microbial community in the inoculum was richer than that in the MEC sample. The OTU number after changing the sulfide concentration increased 5 times unlike the inoculum, where in the community diversity largely increased after the run. This finding was confirmed by the Shannon diversity, Chao1, and ACE indexes, which were higher for MEC sample than in the inoculums sample; by contrast, the Simpson index was lower in the former than in the latter, which further proves the slightly higher diversity of the MEC sample compared with the inoculums sample [27]. The coverage was the same for the MEC sample (0.95) and the inoculum sample (0.95), which indicate that the coverage could sufficiently capture most of the bacterial diversity [28].

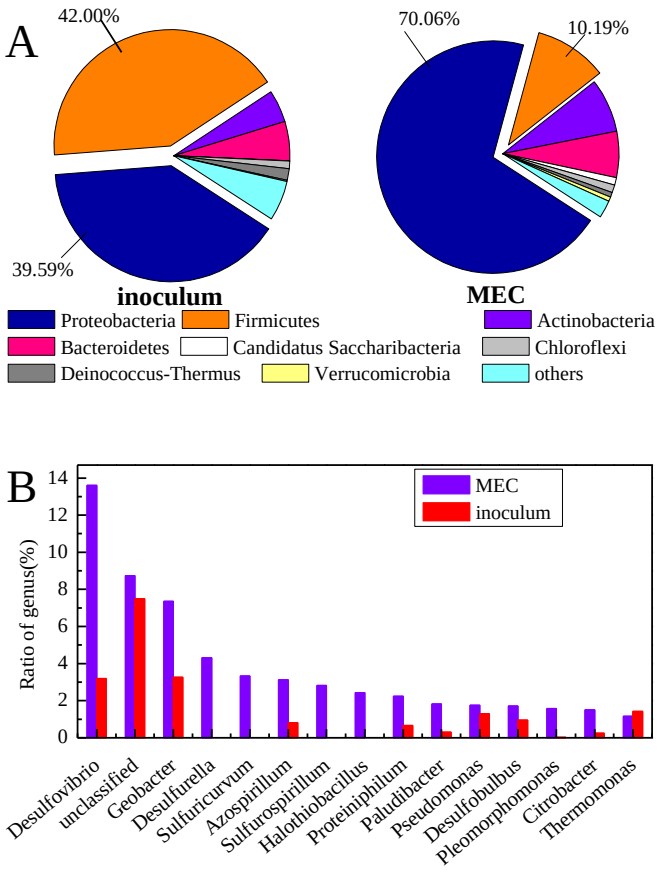

Figure 8. Microbial community distributions for the inoculum and MEC samples with an applied voltage of 0.7 V at (A) the phylum and (B) genus levels.

We analyzed the reads at the phylum level to investigate the different microbial communities. Fig.8A shows that most phyla were similar in the inoculum and MEC samples. *Proteobacteria*, *Firmicutes*, *Actinobacteria* and *Bacteroidetes* were dominant, but with largely different ratios. The bacterial community analysis of the MEC sample revealed the dominance of *Proteobacteria*, which accounted for 70.06% of the biofilm and was significantly higher than that in the inoculum (39.59%). This result is consistent with the results of bacterial communities in active sludge [29], soil [30], and sewage [31]. Furthermore, *Proteobacteria* was the most electrochemically active bacteria, suggesting that electrical stimulation promoted the increase in electroactive bacteria. The frequencies of the phylum *Firmicutes* in the MEC and inoculum samples were 10.19% and 42.00%, respectively. *Firmicutes* was also identified as transferred extracellular electrons in electricity generation [32].

The microbial community distribution at the genus level (Fig.8B) shows that the genera were mainly *Desulfovibrio*(13.61%), *Geobacter*(7.35%), *Desulfurella*(4.31%), *Sulfuricurvum*(3.33%), *Azospirillum*(3.13%), *Sulfurospirillum*(2.82%), and *Halothiobacillus*(2.43%). Results showed a large percentage(8.74%) of *unclassified* species. *Desulfovibrio* was the main bacteria detected in the MEC, which is also the most studied genus of sulfide-related bacteria [33]. *Geobacter* and *Desulfobulbus*, belong to the *Deltaproteobacteria* class. *Deltaproteobacteria* could reportedly enhance the direct electron transfer efficiency between bacteria and the electrode. Wang [34] determined that *Desulfovibrio* is responsible for the direct electron transfer to the electrode. Sulfide removal may occur on the account of *Desulfovibrio* using electrodes that serve as the electron donor. Blázquez [35] also believed that *Desulfovibrio* and *Paludibacter* play key roles in sulfide conversion. The abundance of the genera *Desulfovibrio*, *Geobacter* and *Desulfurella* in the MEC were 13.61%, 7.35%, and 4.31%, respectively, which were considerably higher than those in the inoculums at 3.19%, 3.26%, and 0%, respectively. These results indicate that the bacteria have adapted to the environment.

4. CONCLUSION

This study determined that the optimum concentration of sulfide potassium is 600 $mg \cdot L^{-1}$ for sulfide removal and hydrogen production in the MEC with potassium sulfide as the substrate. Microbial community analysis of the anode biofilm showed a high diversity of bacteria, including *Desulfovibrio*(13.61%), *Geobacter*(7.35%), *Desulfurella*(4.31%), *Sulfuricurvum*(3.33%), *Azospirillum*(3.13%), *Sulfurospirillum*(2.82%), and *Halothiobacillus*(2.43%). These bacteria increased unlike the same bacteria in the inoculum, suggesting that the bacteria have adapted to the environment. *Desulfovibrio* was identified as the bacterial genus responsible for directing the electron transfer to the electrode. This study presents a new and effective method for sulfide removal.

ACKNOWLEDGEMENTS

This work was funded by the Provincial Natural Science Foundations of Shan xi, China(2014011014-6, 2013011009-2). The authors also acknowledge the Institute of Coal Chemistry, Chinese Academy of Sciences for technical assistance.

SUPPLEMENTARY MATERIAL:

1. Hydrogen recovery

Coulombic efficiency (C_E) was calculated on the basis of the measured current compared to the substrate removed using the following Eqs.(1-3):

$$n_{CE} = \frac{\int_0^t Idt}{2F} \quad (1)$$

$$n_{th} = \frac{b_{H_2/S} V_L \Delta C_S}{M_S} \quad (2)$$

$$C_E = \frac{n_{CE}}{n_{th}} \quad (3)$$

Where n_{CE} (mol) is the moles of hydrogen that could be recovered based on measured current, n_{th} (mol) is the maximum theoretical hydrogen potential from the substrate consumption, I (A/m^2) is the current density of the anode surface area, F is the Faraday constant (F=96,485 C/mole$^-$), $b_{H_2/S}$ is the conversion factor of substrate to moles of hydrogen, V_L is the volume of reactor, ΔC_S (g) is the mass of substrate consumption, M_S (g/mol) is the molecular weight of substrate.

The cathodic hydrogen recovery (r_{cat}) was calculated using Eq.(4):

$$r_{cat} = \frac{n_{H_2}}{n_{CE}} \quad (4)$$

Where n_{H2}(mol) is the actual moles of hydrogen recovered at the cathode.

The overall hydrogen recovery (r_{H2}) was calculated using Eq.(5):

$$r_{H_2} = \frac{n_{H_2}}{n_{th}} \quad (5)$$

2. Energy recovery

The electrical energy efficiency (η_w) was calculated using Eq.(6):

$$\eta_w = \frac{\Delta H_{H_2} r_{cat}}{193 E_{ps}} \quad (6)$$

Where $\triangle H_{H2}$ (285.83 kJ/mol) is the energy content of hydrogen based on the heat of combustion, E_{ps}(V) is the applied voltage to the system by the power supply.

The overall energy recovery (η_{w+s}) was calculated using Eq.(7):

$$\eta_{w+s} = \left(\frac{1}{\eta_w} + \frac{\Delta H_S}{\Delta H_{H_2}} \times \frac{1}{\frac{b_{H_2} r_{H_2}}{S}}\right)^{-1} \quad (7)$$

Where $\triangle H_S$ (20.502 kJ/mol) is the energy content of substrate based on the heat of combustion.

The hydrogen production rate (Q_V) was calculated using Eq.(8):

$$Q_{H_2} = 3.68 \times 10^{-5} I_V T r_{cat} \quad (8)$$

Where I_V (A/m^3) is the current density of the liquid volume, T (K) is the temperature.

References

1. E. Vaiopoulou, P. Melidis and A. Aivasidis, *Water. Res.*, 39 (2005) 4101.
2. V. Midha V, M. K. Jha and A. Dey, *J. Environ. Sci-china.*, 24 (2012) 512.
3. Y. Jiang, M. Su and D. Li, *Appl. Biochem. Biotech.*, 172 (2014) 2720.
4. Anaerobic biotechnology for industrial wastewaters, Archae Press, (1996) American.
5. A. H. Nielsen, P. Lens, J. Vollertsen and T. Hvitved-Jacobsen, *Water. Res.*, 39 (2005) 2747.
6. J. Sun, I. Pikaar, K. R. Sharma, J. Keller and Z. Yuan, *Water. Res.*, 71 (2015) 150.
7. I. B. Hariz and L. Monser, *International Water Technology Journal.*, 4 (2014) 264.
8. L. Zhang, P. De Schryver, B. De Gusseme, W. De Muynck, N. Boon and W. Verstraete, *Water. Res.*, 42 (2008) 1.
9. M. Sun, Z. X. Mu, Y. P. Chen, G. P. Sheng, X. W. Liu, Y. Z. Chen, Y. Zhao, H. L. Wang, H. Q. Yu, L. Wei and F. Ma, *Environ. Sci. technol.*, 43 (2009) 3372.

10. K. Rabaey, K. Van de Sompel, L. Maignien, N. Boon, P. Aelterman, P. Clauwaert, L. De Schamphelaire, H. T. Pham, J. Vermeulen, M. Verhaege, P. Lens and W. Verstraete, *Environ. Sci. technol.*, 40 (2006) 5218.
11. K. Guo, A. Prévoteau and K. Rabaey, *J. Power. Sources.*, 356 (2017) 484.
12. H. Zhao, Y. Zhang, B. Zhao B, Y. Y. Chang and Z. S. Li, *Environ. Sci. technol.*, 46 (2012) 5198.
13. Y. X. Zhang, L. Z. Tang, Y. F. Deng and S. Z. Zhan, *Inorg. Chem. Commun.*, 72 (2016) 100.
14. G. Kumar, P. Bakonyi, T. Kobayashi, K. Q. Xu, P. Sivagurunathan, S. H. Kim, G. Buitrón, N. Nemestóthy and K. Bélafi-Bakó, *Renew. Sust. Energ. Rev.*, 57 (2016) 879.
15. H. Lin, N. Williams, A. King A and B. Hu, *Chem. Eng. J.*, 297 (2016) 180.
16. H. Dai, H. Yang, X. Liu, Y. Zhao and Z. Liang, *Bioresource technol.*, 202 (2016) 220.
17. Standard methods for the examination of water and wastewater, American Public Health Association, American Water Works Association, Water Pollution Control Federation, & Water Environment Federation, American, 1915, Vol. 2.
18. H. Dai, H. Yang, X. Liu, X. Jian and Z. Liang, *Fuel.*, 174 (2016) 251.
19. H. Liu, B. Zhang, Y. Liu, Z. Wang and L. Hao, *Int. J. Hydrogen energy.*, 40 (2015) 8128.
20. B. Zhang, J. Zhang, Y. Liu, C. Hao, C. Tian, C. Feng, Z. Lei, W. Huang and Z. Zhang, *Int. J. Hydrogen energy.*, 38 (2013) 14348.
21. Y. Gong, A. Ebrahim, A. M. Feist, M. Embreet, T. Zhang, D. Lovley and K. Zengler, *Environ. Sci. technol.*, 47 (2012) 568.
22. M. Su, L. Wei, Z. Qiu, G. Wang and J. Shen, *J. Power. Sources.*, 301 (2016) 29.
23. A. Ghimire, L. Frunzo, F. Pirozzi, E. Trably, R. Escudie, P. N. Lens and G. Esposito, *Appl. Energ.*, 144 (2015) 73.
24. M. Mehanna, P. D. Kiely, D. F. Call and B. E. Logan, *Environ. Sci. technol.*, 44 (2010) 9578.
25. L. Lu, D. Hou, Y. Fang, Y. Huang and Z. J. Ren, *Electrochim. Acta.*, 206 (2016) 381.
26. M. Mitov, E. Chorbadzhiyska, L. Nalbandian L and Y. Hubenova, *J. Power. Sources.*, 356 (2017) 467.
27. E. M. Fykse, T. Aarskaug, E. H. Madslien and M. Dybwad, *Bioresource technol.*, 222 (2016) 380.
28. M. Sun, Z. H. Tong, G. P. Sheng, Y. Z. Chen, F. Zhang, Z. X. Mu, H. L. Wang, R. J. Zeng, X. W. Liu, H. Q. Yu, L. Wei and F. Ma, *Biosens. Bioelectron.*, 26 (2010) 470.
29. T. Zhang, M. F. Shao and L. Ye, *Isme J.*, 6 (2012) 1137.
30. L. F. W. Roesch, R. R. Fulthorpe, A. Riva, G. Casella, A. K. M. Hadwin, A. D. kent, S. H. Daroub, F. A. O. Camargo, W. G. Farmerie and E. W. Triplett, *Isme J.*, 1 (2007) 283.
31. S. L. McLellan, S. M. Huse, S. R. Mueller-Spitz, E. N. Andreishcheva and M. L. Sogin, *Environ. Microbial.*, 12 (2010) 378.
32. J. Huang, Z. Wang, C. Zhu, J. Ma, X. Zhang and Z. Wu, *PloS one.*, 9 (2014): e93842.
33. T. Hao, P. Xiang, H. R. Mackey, K. Chi, H. Lu, H. Chui, M. C. M. Van Loosdrecht and G. Chen, *Water. Res.*, 65 (2014) 1.
34. K. Wang, Y. Sheng, H. Cao, K. Yan and Y. Zhang, *Chem. Eng. J.*, 307 (2017) 150.
35. E. Blázquez, D. Gabriel, J. A. Baeza and A. Guisasola, *Water. Res.*, 105 (2016) 395.